

Accepted Manuscript

Measurement of single electron emission in two-phase xenon

B. Edwards, H.M. Araújo, V. Chepel, D. Cline, T. Durkin, J. Gao, C. Ghag, E.V. Korolkova, V.N. Lebedenko, A. Lindote, M.I. Lopes, R. Lüscher, A.St.J. Murphy, F. Neves, W. Ooi, J. Pinto da Cunha, R.M. Preece, G. Salinas, C. Silva, V.N. Solovov, N.J.T. Smith, P.F. Smith, T.J. Sumner, C. Thorne, R.J. Walker, H. Wang, J.T. White, F.L.H. Wolfs

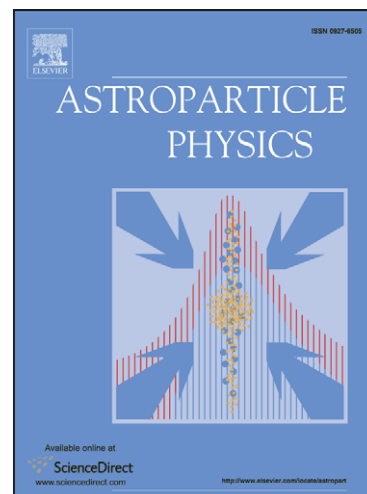
PII: S0927-6505(08)00078-9
DOI: [10.1016/j.astropartphys.2008.06.006](https://doi.org/10.1016/j.astropartphys.2008.06.006)
Reference: ASTPHY 1315

To appear in: *Astroparticle Physics*

Received Date: 14 December 2007
Revised Date: 25 March 2008
Accepted Date: 12 June 2008

Please cite this article as: B. Edwards, H.M. Araújo, V. Chepel, D. Cline, T. Durkin, J. Gao, C. Ghag, E.V. Korolkova, V.N. Lebedenko, A. Lindote, M.I. Lopes, R. Lüscher, A.St.J. Murphy, F. Neves, W. Ooi, J. Pinto da Cunha, R.M. Preece, G. Salinas, C. Silva, V.N. Solovov, N.J.T. Smith, P.F. Smith, T.J. Sumner, C. Thorne, R.J. Walker, H. Wang, J.T. White, F.L.H. Wolfs, Measurement of single electron emission in two-phase xenon, *Astroparticle Physics* (2008), doi: [10.1016/j.astropartphys.2008.06.006](https://doi.org/10.1016/j.astropartphys.2008.06.006)

This is a PDF file of an unedited manuscript that has been accepted for publication. As a service to our customers we are providing this early version of the manuscript. The manuscript will undergo copyediting, typesetting, and review of the resulting proof before it is published in its final form. Please note that during the production process errors may be discovered which could affect the content, and all legal disclaimers that apply to the journal pertain.



Measurement of single electron emission in two-phase xenon

B.Edwards,^{1,2} H.M.Araújo,^{1,2} V.Chepel,³ D.Cline,⁴ T.Durkin,² J.Gao,⁵
 C.Ghag,⁶ E.V.Korolkova,⁶ V.N.Lebedenko,¹ A.Lindote,³ M.I.Lopes,³
 R.Lüscher,² A.St.J.Murphy,⁶ F.Neves,³ W.Ooi,⁴ J.Pinto da Cunha,³
 R.M.Preece,² G.Salinas,⁵ C.Silva,³ V.N.Solovov,³ N.J.T.Smith,² P.F.Smith,^{2,4}
 T.J.Sumner,¹ C.Thorne,¹ R.J.Walker,¹ H.Wang,⁴ J.T.White,⁵ and F.L.H.Wolfs⁷

¹*Blackett Laboratory, Imperial College London, UK*

²*Particle Physics Dept., Rutherford Appleton Laboratory, UK*

³*LIP-Coimbra & Department of Physics of the University of Coimbra, Portugal*

⁴*Department of Physics & Astronomy,
 University of California, Los Angeles, USA*

⁵*Department of Physics, Texas A&M University, USA*

⁶*School of Physics, University of Edinburgh, UK*

⁷*Department of Physics and Astronomy,
 University of Rochester, New York, USA*

(Dated: July 2, 2008)

Abstract

We present the first measurements of the electroluminescence response to the emission of single electrons in a two-phase noble gas detector. Single ionization electrons generated in liquid xenon are detected in a thin gas layer during the 31-day background run of the ZEPLIN-II experiment, a two-phase xenon detector for WIMP dark matter searches. Both the pressure dependence and magnitude of the single-electron response are in agreement with previous measurements of electroluminescence yield in xenon. We discuss different photoionization processes as possible cause for the sample of single electrons studied in this work. This observation may have implications for the design and operation of future large-scale two-phase systems.

PACS numbers: 61.25.Bi, 78.60.Fi, 95.35.+d, 29.40.Mc

Keywords: ZEPLIN-II, liquid xenon, electroluminescence, radiation detectors

Early work investigating two-phase emission of ionization electrons was carried out in the 1940's [1], but the mechanism was not fully exploited as a method for radiation detection until the 1970s with the development of detectors using condensed argon [2]. Application of the two-phase technique has since expanded into highly-demanding areas, most notably WIMP dark matter searches [3–7], with coherent neutrino scattering and double β -decay experiments proposed [8–10].

In two-phase xenon, a particle interacting in the liquid xenon (LXe) target produces prompt scintillation photons [11, 12] in the vacuum ultra-violet (VUV) with $\lambda \simeq 175 \pm 7$ nm [13, 14]. At zero electric field, ionization electrons created by the interaction will recombine, increasing the scintillation signal. By applying an external field to the liquid, some electrons can be extracted from the interaction site to be detected independently. The currently favoured method of charge detection from a liquid target relies on using electroluminescence to convert the ionization signal into a proportional photon yield in the gas phase [15]. Upon reaching the liquid surface, electrons can be emitted into the gas phase with near unity efficiency at 5 kV/cm [16]. Once in the gas, they are accelerated by the stronger field there, collisionally exciting atoms to produce secondary VUV scintillation photons. This electroluminescence process has been studied previously [17–22], although some disagreement remains over the absolute number of photons produced per electron.

Presented here is the first study quantifying the response to the cross-phase emission of a single ionization electron in a noble gas detector. In two-phase argon, a three-stage Gas Electron Multiplier (GEM) has recently been reported to achieve single-electron sensitivity, although this study relied on electrons photo-produced in the first GEM in the gas rather than emitted from the liquid [23]. Sensitivity to single ionization electrons is important in experiments searching for very small, rare events. On a technical level, it allows for direct measurement of the ionization yields of different interacting particles, such as nuclear and electron recoils, and may help with the study of photoionization processes in LXe. Understanding the origin of these electrons may highlight new backgrounds for experiments relying on the detection of even smaller ionization signatures than those considered of interest in WIMP dark matter searches, which motivated this study. One such example is the proposed detection of keV energy deposits from coherent neutrino scattering [8].

This work was carried out using ZEPLIN-II, a two-phase xenon detector searching for WIMP dark matter. Its 31 kg LXe target is held in a truncated cone of reflective Polyte-

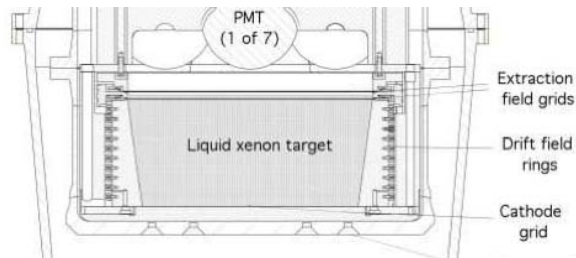


FIG. 1: Schematic of the ZEPLIN-II detector. The liquid and gaseous xenon regions are shown, along with the electric field electrodes and the array of PMTs detecting VUV photons.

trafluoroethylene (PTFE), 140 mm deep, with upper and lower diameters of 324 mm and 290 mm (Fig. 1). The liquid surface lies between two meshes 10 mm apart, where a strong electric field can be applied to produce electroluminescence from emitted electrons. Details of the detector design, operation and primary analysis can be found in Ref. [4]. The extraction electrodes consist of a woven stainless steel mesh of 30 μm wire, at a separation of 500 μm . Electrons are drifted towards the extraction region by a vertical 1 kV/cm field; upon reaching the surface, they are emitted into the gas by an electric field of ~ 4.8 kV/cm and accelerated across the 2-3 mm gas gap by a field twice as strong. Both the primary (scintillation) and secondary (electroluminescence) signals are independently detected by seven photo-multiplier tubes (PMTs). The time taken for the electrons to drift through the liquid provides a separation in time proportional to the depth in the detector.

Data from the 31-day shielded run of ZEPLIN-II was searched for evidence of single electron emission. During this run the average background rate from γ -ray interactions was ~ 2 evt/s (>5 keV). An unexpected population of very small secondary-like signals immediately following large secondaries was apparent during early tests. Some of these signals were also observed *between* the primary and secondary pulses associated with normal events and these were selected for further analysis.

The detector response to a single emitted electron is predicted to be small, yielding fewer than 10 photoelectrons across the PMT array. To search for such small signals, quiet timelines free from spurious noise, overlapping events and optical feedback effects are required. For this reason the search for candidate single electron signals was carried out on the low-background dataset used for WIMP searches. From this dataset, only events triggered by the primary scintillation signal were selected in order not to bias the size of the candidate signals. The trigger function is a 5-fold coincidence above $1/3$ of a single PMT photoelectron

(phe) ($\gtrsim 80\%$ efficiency per channel) within a narrow coincidence window. This lowers the absolute trigger efficiency for single electrons, which minimises the impact on data volume. For this reason, the absolute rate of single electrons in the dataset cannot be calculated, only the rate relative to primary scintillation triggers.

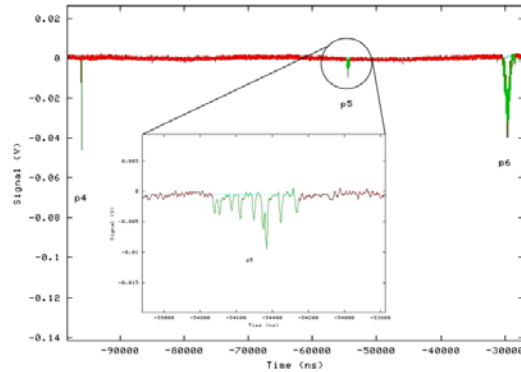


FIG. 2: Seven-PMT sum waveform containing a candidate single electron signal (p5) visible between the primary scintillation pulse (p4) and the electroluminescence pulse (p6).

Fig. 2 shows a typical $80\ \mu\text{s}$ waveform (sampled at $2\ \text{ns}$) containing a primary scintillation pulse and a secondary electroluminescence pulse, with a single electron candidate observed in the intervening time. The latter is detected as a collection of individual PMT photoelectrons spread over a $\sim 500\ \text{ns}$ period, the time required for electrons to cross the high-field gas region.

In the analysis described in Ref. [4], the data were corrected for the finite electron lifetime in the LXe as well as operational parameters which affect the gain of the ionization channel (such as variations of pressure, liquid level and electric fields). In this analysis the ‘purity’ correction, compensating the secondary signal for electron trapping by electronegative impurities during their drift to the surface, is not required as a single electron will either reach the surface or be trapped, meaning no *partial* loss of signal. The other operational parameters are considered as variables.

A pulse area histogram of all small signals detected between primary and secondary pulses is shown in Fig. 3. The mean spe area for each PMT is independently measured. The figure shows a clear population which we attribute to single electrons, along with an exponential noise pedestal. The distribution of single electrons is fitted with a Gaussian. Although phe statistics suggest a Poisson distribution, further broadening occurs due to electronic noise and other fluctuations. The spectrum shows the single electron mean of 8.8 ± 0.4 phe and a

width $\sigma=5.0$ phe, a gain of over 200 VUV photons/electron, as discussed later.

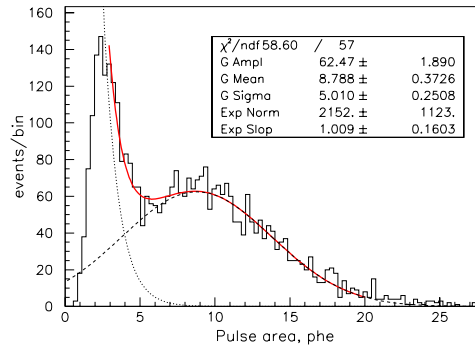


FIG. 3: Single electron spectrum at 1.5 bar gas pressure. The continuous line shows the fit to the entire spectrum; the Gaussian and exponential components are also shown. The inset shows the Gaussian plus exponential fit parameters.

The number of electroluminescence photons created per electron depends on the pressure, electric field and gas thickness. The electroluminescence yield of xenon, i.e. the number of VUV photons produced per electron per cm travelled, has been studied mainly for room-temperature gas (see [22] and references therein). A dependence is found of the form $Y = aE - bP_{eq}$, where a and b are experimental parameters, E is the field in the gas and P_{eq} is the equivalent pressure for the same gas density at 0°C . It is known that the photon yield in the cold, saturated vapour is higher than that in the warm gas (for the same density). This effect is clearly shown in Ref. [20], where the room temperature measurement is consistent with other published results, but the yield in the vapour is clearly higher. We note that for the mesh design and thickness of the gas layer mentioned previously, a parallel and uniform electric field can be assumed without significant error. This allows calculation of the absolute yield in ZEPLIN-II. If the small signals under scrutiny correspond to the emission of a single electron, this yield must agree with that measured for the cold vapour and show the same pressure dependence.

Gas pressure, P , is a key operational parameter affecting the single electron response, doing so in two complementary ways: it affects electroluminescence at a microscopic level and is also directly linked to the liquid level through thermal expansion of the liquid, which is in thermal equilibrium with the gas. Thermal expansion causes only a small variation of the field in the gas. Previous yield measurements can be compared directly with ZEPLIN-II

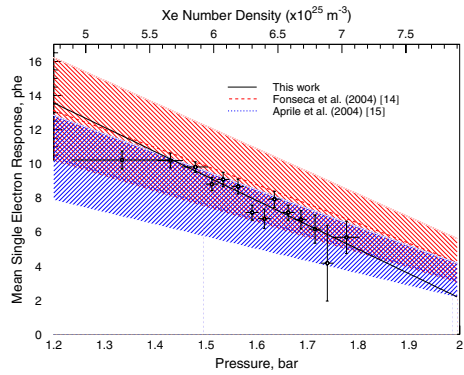


FIG. 4: Dependence of single electron response on detector pressure, compared with predictions from previous measurements of electroluminescence yield in saturated vapour. The shaded bands represent uncertainties assigned to these predictions, including an ad-hoc 10% error assumed for parameters a and b (not given in the literature).

results by factoring in the thickness of the gas region, d , the light collection efficiency, $\eta=0.24$, and the PMT quantum efficiencies, $QE \simeq 0.17$. The gas thickness is calculated from the drift time of background interactions occurring very near the lower extraction grid just under the surface; the light collection was simulated by Monte Carlo; there is some uncertainty about the variation of PMT QE down to low temperatures for this particular phototube model, but we believe it to be small. Fig. 4 shows the mean single electron response (in phe), $QE \eta d(P) Y(P)$, demonstrating the expected dependence with pressure over the range 1.2–1.9 bar, the variation observed during this run. Both the number of photons and the pressure behaviour agree well with predictions based on independent measurements of the absolute yield and, combined, provide strong evidence that the candidate population is indeed from single electrons.

The ZEPLIN-II position reconstruction in the horizontal plane lacks precision for signals as small as those considered here. However, the reconstructed radial distribution shown in Fig. 5 is consistent with generation over all radii, which is clearly incompatible with that of small ionization signals originating from the detector walls (corresponding to a radius of $r=0.7$ a.u.). The latter is a known background of nuclear recoils arising from plating of the PTFE walls with α -emitters from ^{222}Rn decay in the LXe [4]. The depth (drift time) distribution also shows relatively uniform production throughout the LXe bulk.

The fact that large secondaries appear to be followed by multiple single electron pulses

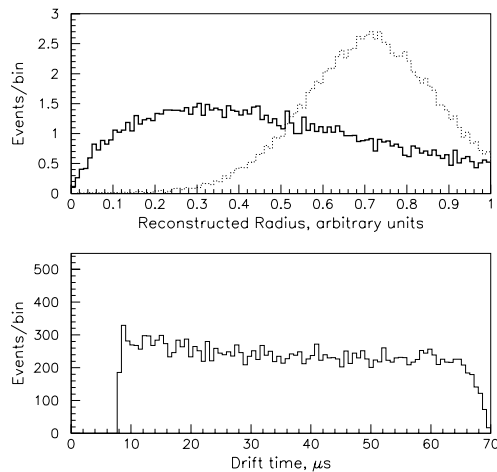


FIG. 5: Radial (top) and depth (bottom) distributions. In the top plot the solid line shows the single electron population and the dashed line the distribution of small ionization signals (\sim few electrons) from detector walls (Rn-induced events) [4].

suggests their production may be related to the number of VUV photons in the chamber. The quiet timelines found between primary and secondary signals, together with the proportionality between the primary signal and the energy deposited, allow testing of this hypothesis in a quantitative manner. Fig. 6 shows the fraction of events where a single electron is observed as a function of energy (proportional to the number of scintillation photons generated in the liquid). A clear energy dependence is observed, suggesting that the production of single electrons could be, at least in part, due to photoionization processes in the liquid.

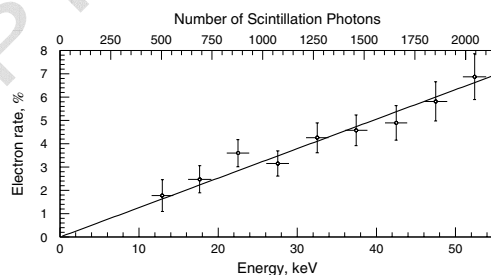


FIG. 6: Fraction of primary triggers where a single electron is observed as a function of primary signal size (normalized to γ -ray energy), calculated as the fraction of timelines checked containing single electron signals.

The mean free path (mfp) of the $\simeq 7.1$ eV photons for generating an electron in LXe can be estimated from Fig. 6. Combining the slope of the trend line with a scintillation yield of 39 photons/keV (measured at 1 kV/cm), we conclude that an average of 32,500 photons are required to produce an electron. These photons can escape from the surface or be absorbed in the surrounding PTFE or in the electrodes. A Monte Carlo simulation places the mean escape length from the LXe at ~ 25 cm for photons generated uniformly. This value is not significantly affected by bulk absorption for the xenon purity considered here, or by Rayleigh scattering. This places the photon mfp for photoionization at $\sim 1.0 \times 10^6$ cm. Several chemical species, including xenon itself, can be responsible, but impurities in the liquid are the most likely. Unfortunately, the mfp depends on both the microscopic cross-section and the atom number density, and so none can be ruled out with certainty since either (or both) quantities may be unknown.

Sub-threshold photoionization, either of impurities or of Xe atoms, dimers and higher order polymers, cannot be ruled out, even if it is unlikely. Some of the most abundant impurities are electronegative species (e.g. O_2 , H_2O , N_2O , etc) responsible for the finite electron lifetime. Although these have ionisation energies typically above 12 eV in gas phase [24], this does not rule out completely the possibility of photoionisation at lower energies. Their concentration can be estimated from the rate of electron attachment. From known attachment cross-sections [25] at an average energy of 0.1 eV for electrons drifting in a 1 kV/cm field [26], we estimate that an O_2 concentration of ~ 60 ppb or a N_2O at just ~ 8 ppb would produce the $\sim 100 \mu s$ electron lifetime observed during this run. The photoionization cross-section needed to explain the measured mfp is only ~ 0.001 Mb (compared to 10-100 Mb typically found well above threshold). During the data run, the electron lifetime did not vary enough to allow us to study any possible correlation with the single electron production rate.

In the case of intrinsic LXe photoionization (9.3 eV threshold [27]) a cross-section as low as $35 \mu b$ is sufficient. So, although the sub-threshold process is very unlikely, the interaction probabilities required are also extremely small; in addition, the non-zero width of the scintillation emission will play a favourable role.

Alternatively, minute amounts of species with low ionization thresholds may be responsible, of which there are many candidates, organic and inorganic. In addition to neutral species, it is also conceivable that negative ions previously created by electron attachment

can be photoionised during their long drift towards the anode, which is as slow as ~ 0.7 cm/s for a O_2^- ions in LXe [28]. However, the concentration of O_2^- accumulated from electron attachment during calibration and background runs seems too low to explain the observed rate. Finally, we mention photoionization induced by the well-known ‘n=1’ LXe exciton, which lies below the intrinsic threshold at 8.4 eV [29–31]. Although excitons do not cause photoionization directly, they can transfer the excitation to impurities onto which they become trapped and ionise them in a Penning-type interaction.

In summary, a population of small signals in the ZEPLIN-II data was identified with the emission of single electrons into the gas region, probably caused by photoionization of a yet underdetermined contaminant species in the LXe. The detection of single electrons demonstrates the excellent sensitivity of the ionization channel in two-phase xenon systems.

The authors would like to thank the ZEPLIN-II collaboration. Thanks are also due to D. Akimov (ITEP, Moscow) for useful discussions. This work was funded by the UK Particle Physics and Astronomy Research Council (PPARC), the Portuguese FCT (POCI/FP/FNU/63446/2005), the US DOE (# DE-FG03-91ER40662) and NSF (# PHY-139065).

-
- [1] G.W.Hutchinson, *Nature* 162, 4120 (1948).
 - [2] B.A.Dolgoshein, V.N.Lebedenko, B.U.Rodionov, *JETP Lett.* 11, 351 (1970).
 - [3] D.Y.Akimov, *Instr. Exp. Tech.* 44, 575 (2001).
 - [4] G.J.Alners *et al.*, *Astroparticle Phys.* 28(3) 287 (2007)
 - [5] D.Yu.Akimov *et al.*, *Astroparticle Phys.* 27(1) 46 (2007)
 - [6] J.Angle *et al.*, *Phys. Rev. Lett.* 100, 021303 (2008)
 - [7] P.Benetti *et al.*, *Astroparticle Phys.* 28(6), 495 (2008)
 - [8] C.Hagmann & A.Bernstein, *IEEE Trans. Nucl. Sci.* 51, 2151 (2004).
 - [9] K.Scholberg, *Phys. Rev. D* 73, 033005 (2006).
 - [10] A.Bueno *et al.*, *Phys. Rev. D* 74, 033010 (2006).
 - [11] S.Kubota *et al.*, *Phys. Rev. B* 20(8), 3486 (1979).
 - [12] A.Hitachi *et al.*, *Phys. Rev. B* 27(9), 5279 (1983).
 - [13] E.Morikawa *et al.*, *J. Chem. Phys.* 91(3), 1469 (1989).

- [14] A. Hitachi *et al.*, Nucl. Instrum. Methods 196 (1982).
- [15] A.Bolozdynya, Nucl. Instr. Meth. A 422, 314 (1999).
- [16] E.M.Gushchin *et al.*, Sov.Phys. JETP. 49(5), 856 (1979).
- [17] C.A.N.Conde *et al.*, Trans. Nucl. Sci. NS-24, 221 (1977).
- [18] F.P.Santos *et al.*, J. Phys. D: Appl. Phys. 27, 42 (1994).
- [19] D. Yu. Akimov *et al.*, Phys. At. Nuc. 61(7), 1341 (1998).
- [20] A.C.Fonseca *et al.*, IEEE Trans. Nucl. Sci. 1, 572 (2004)
- [21] E.Aprile *et al.*, IEEE Trans. Nucl. Sci. 51(5), 1986 (2004)
- [22] C.M.B. Monteiro *et al.*, astro-ph/0702142
- [23] A.Bondar *et al.*, arXiv:physics/0611068v1
- [24] CRC Handbook of Chemistry and Physics, 88th Edition 2007-2008
(http://www.hbcnetbase.com/articles/10_06_86.pdf)
- [25] G.Bakale, U.Sowada & W.F.Schmidt, J. Phys. Chem. 80(23), 2556 (1976).
- [26] E.M.Gullikson & B.L.Henke, Phys. Rev. B 39(1), 1 (1989).
- [27] R.Reininger *et al.*, Phys. Rev. B 28(6), 3193 (1983).
- [28] W.F.Schmidt, O.Hilt, E.Illenberger & A.G.Khrapak, Rad. Phys. Chem. 74, 152 (2005).
- [29] D.Beaglehole, Phys. Rev. Lett. 15(13), 551 (1965).
- [30] M.Reshotko *et al.*, Phys. Rev. B 43(17), 14174 (1991).
- [31] A.Hitachi, J. Chem. Phys. 80(2), 745 (1984).